Improving the Performance of a Non-Volatile Magnetic Flip Flop by Exploiting the Spin Hall Effect

Thomas Windbacher, Alexander Makarov, Viktor Sverdlov, and Siegfried Selberherr
Institute for Microelectronics, TU Wien, Gußhaustraße 27–29/E360, A–1040 Wien, Austria
Email: {windbacher|makarov|sverdlov|selberherr}@iue.tuwien.ac.at

***Abstract*—The introduction of non-volatile elements into state-of-the art computing systems is a promising way to circumvent power dissipation and interconnection delay bottlenecks. This led us to the proposal of a non-volatile magnetic flip flop which offers high integration density as well as CMOS compatibility by not only acting as an auxiliary memory element but also carrying out the actual computation in the magnetic domain without relying on additional CMOS components. However, the required switching energy is still relatively high which results in a high current density needed for the flip flop manipulation. Here, we propose a modified device structure with a different device operation principle to benefit from the spin Hall effect in order to reduce the required switching energy without degrading other important parameters like switching speed or device reliability. Our results show that the use of the spin Hall effect is rewarded by a simultaneous reduction in switching time ($\times 5 - \times 2$) and switching energy ($\times 5 - \times 1.6$).**

I. Introduction

CMOS scaling was the key for competitiveness in the semiconductor market for many decades [1]. It allowed to manufacture inexpensive electronics with increased performance for each new technology generation. It also caused a perpetual fight to keep control over the channel in CMOS transistors and led to the continuous introduction of innovations in CMOS processes, materials, and device structures like local and global strain techniques, high-k/metal gates, and Tri-gate FETs. Nowadays the static power consumption growth and the interconnection delay increase for each new technology node are among the most pressing obstacles [2].

A simple but powerful solution to this problem is to shut down unused circuit parts and only power them when they are needed. Since the information previously held by the dormant circuit will be lost when it is turned on again, its last state has to be re-established. This requires to copy the lost information back, which again is disadvantageous with respect to interconnection delay and dissipated power. Therefore, the transition towards normally "Off" circuits induces the introduction of non-volatility into the circuits and thereby a redesign of all basic building blocks in CMOS.

Spin as a degree of freedom and its utilization for spin-based devices is very appealing, due to its non-volatility, fast operation, and high endurance [3]. Currently the most mature and also commercially available solutions which exploit spintronics are mainly supplements and sometimes only replacements for static and dynamic embedded CMOS-based memory [4], [5].

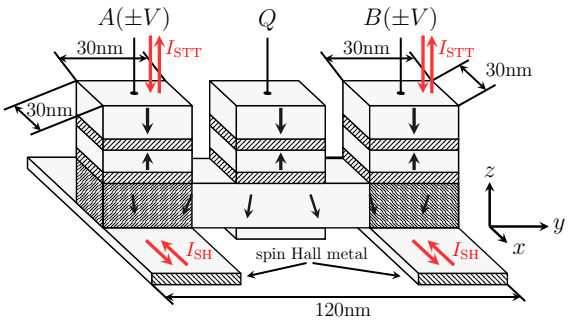

Fig. 1. The non-volatile magnetic flip flop consists of three anti-ferromagnetically coupled polarizer stacks (A, B, and Q), which are connected via a common free layer. The common free layer resides on two spin Hall metal lines.

Nevertheless several challenges remain, like the up to now rather high current density required to switch the magnetization orientation of the free magnetic layer and the decreasing thermal stability, when magnetic tunnel junctions (MTJ) are shrunk. Although scaled down CMOS logic transistors still outperform MTJ devices with respect to switching energy [3], innovations, i.e. the introduction of perpendicular magnetic anisotropies in conjunction with MgO tunnel barriers, diminishes the switching energy to a degree such that it is able to compete with CMOS SRAM cache [6], [7], [8].

Up to now the non-volatility is commonly introduced into logic circuits by using magnetic tunnel junctions which act as auxiliary devices holding only the information, while the necessary processing is carried out by CMOS components [9]. This commonly leads to a decrease in the integration density, since extra components are needed to convert the signals between the resistance state of the MTJs and the voltage or current signals every time data is saved or read, and thus makes it expensive for large scale integration. Therefore, we have proposed a novel non-volatile magnetic flip flop which not only holds the information in the magnetic domain but carries out the logic operations via the spin transfer torque effect, thus enabling denser and simpler layouts as well as harvesting the beneficial features related to spintronics [10].

Nevertheless, as mentioned previously, the required switching energy must be further improved without degrading the switching speed or device reliability to improve the competitiveness of the device. A possible path to realize this is the

978-1-4673-7860-4/15/$31.00 ©2015 IEEE

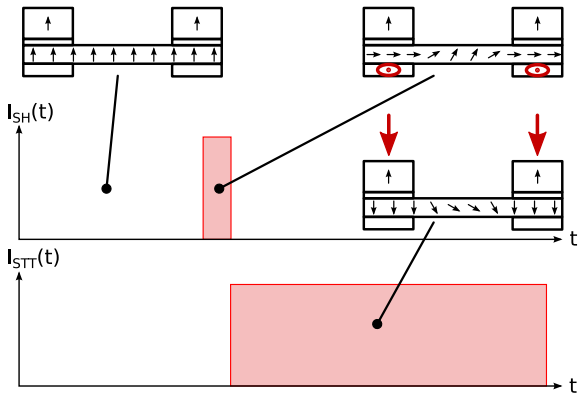

Fig. 2. The flip flop is operated by a first current pulse through the spin Hall metal lines and subsequent current pulses through the polarizer stacks A and B. Due to the high efficiency of the spin Hall effect in $\beta - W$ [15] the required switching time as well as the switching energy can be significantly reduced.

exploitation of the spin Hall effect (SHE) for switching [11], [12], [13], [14].

II. Idea and Operation Principle

To benefit from the SHE, we propose an adapted structure consisting of three anti-ferromagnetically coupled magnetic stacks with out-of-plane magnetization, which are connected to a common free magnetic layer with a perpendicular anisotropy by magnesium oxide layers. The common free layer is placed on two spin Hall metal lines (see Fig. 1). The logic information is mapped to the magnetic orientation of the free layer and can be SET/RESET by applying first a short pulse through the spin Hall metal lines and a subsequent pulse through the polarizer stacks A and B (shown in Fig. 2). The stored information is accessible either by measuring the resistance of one of the stacks (i.e. the readout stack Q) via the giant magnetoresistance or tunneling magnetoresistance effect (e.g. $High/Low \rightarrow 1/0$) or by using the free layer as a polarizer for a subsequent stage [16].

The current pulses through the spin Hall metal lines generate a spin accumulation with an in-plane orientation at their interfaces adjacent to the free layer, which creates spin transfer torques that push the magnetization orientation of the free layer in-plane (cf. (5)). The subsequent current pulses through the polarizer stacks A and B lead to spin transfer torques acting out-of-plane and are necessary to tilt the magnetization into the desired relaxation direction. In order to switch the non-volatile flip flop two input pulses (input stacks A and B) with identical torque directions (identical polarities) are needed. In the case of opposing polarities the exerted spin torques in the corresponding portion of the free layer of the input stacks act against each other and the magnetization is kept in its current state. Thus, a sequence of sufficiently high and long enough pulses with identical polarity either write logic 0 or 1 into the common free layer (RESET/SET), while a sequence with opposing polarities cancel each other and the initial magnetization state is held (HOLD). This corresponds to the logic behavior of a flip flop [10], [17].

Parameter	Value
Free layer length	120nm
Free layer width	30nm
Free layer thickness	2nm
Contact size a	$30\text{nm} \times 30\text{nm}$
Magnetization saturation M_S	$4 \times 10^5 \text{A/m}$
Out-of-plane uni-axial anisotropy K_1	$2 \times 10^5 \text{J/m}^3$
Uniform exchange constant A_{exch}	$2 \times 10^{-11} \text{J/m}$
Polarization P	0.3
Resistance area product $\mathcal{RA}$ of MTJ	$7\,\Omega\mu\text{m}^2$
Gilbert gyromagnetic ratio γ	$2.211 \times 10^5 \text{m/As}$
Damping constant α	0.01
Spin Hall metal ($\beta - W$) cross section	$30\text{nm} \times 3\text{nm}$
Spin Hall angle θ_{SH}	0.3
Spin Hall resistivity ρ_{SH}	$200\mu\Omega\text{cm}$
Non-adiabatic spin Hall contribution ϵ	0.01
Spin flip length λ_{SF}	1.4nm
Spin Hall pulse length	50ps
Spin transfer torque pulse length	10ns
Discretization length Δx, Δy, Δz	2nm
Discretization time Δt	$2 \times 10^{-14} s$

TABLE I. Simulation Parameters

III. Simulation Setup and Theory

We carried out an extensive set of simulations for the proposed device. The current density through the polarizer stacks A and B was fixed at $1.7 \times 10^{11} \text{A/m}^2$ where the flip flop safely operated without spin Hall torque. Then the spin Hall current was varied from 0 up to 5mA to investigate the influence of the spin Hall torque on the switching time and energy. Each data point shown in Fig. 3, Fig. 4, and Fig. 5 depicts an average over 100 samples. The free layer was assumed $30\text{nm} \times 120\text{nm} \times 2\text{nm}$ $CoFeB$ [18] and the cross section of the spin Hall $\beta - W$ lines was defined as $30\text{nm} \times 3\text{nm}$ [19]. Furthermore, the stray fields from the anti-ferromagnetically coupled polarizer stacks were considered negligible. A detailed listing of the employed parameters is given in Tab. I.

The dynamics of the studied non-volatile magnetic flip flops is governed by the Landau-Lifshitz-Gilbert equation [20], [21] supplemented with terms for the torques caused by the spin transfer $\vec{T}_{STT}$ and the spin Hall effect $\vec{T}_{SH}$:

$$\frac{\mathrm{d}}{\mathrm{d}t}\vec{m} = \gamma \left(-\vec{m} \times \vec{H}_{\text{eff}} + \alpha \left(\vec{m} \times \frac{\mathrm{d}}{\mathrm{d}t}\vec{m} \right) + \vec{T}_{STT} + \vec{T}_{SH} \right) \quad (1)$$

$\vec{m}$ denotes the reduced magnetization, γ the electron gyromagnetic ratio, α the dimensionless damping constant, and $\vec{H}_{eff}$ the effective field. The precessional motion due to the effective magnetic field $\vec{H}_{\text{eff}}$ is described by the first term in (1). A power dissipation proportional to $\frac{\mathrm{d}}{\mathrm{d}t}\vec{m}$ is introduced by the second term and the effective field $\vec{H}_{\text{eff}}$ contains contributions from the uni-axial anisotropy, exchange, and demagnetization energy as well as thermal excitations [22], [23], [24].

In the non-magnetic layers made out of magnesium oxide the spin transfer torque $\vec{T}_{STT}$ is modeled by the following expression [25]:

$$\vec{T}_{STT} = \frac{\hbar}{\mu_0 e} \cdot \frac{J}{l M_S} \cdot \frac{P}{2\,(1 + P^2\,(\vec{m} \cdot \vec{p}))} \cdot \cdot \left(\vec{m} \times \vec{p} \times \vec{m} - \alpha\, \vec{m} \times \vec{p} \right) \quad (2)$$

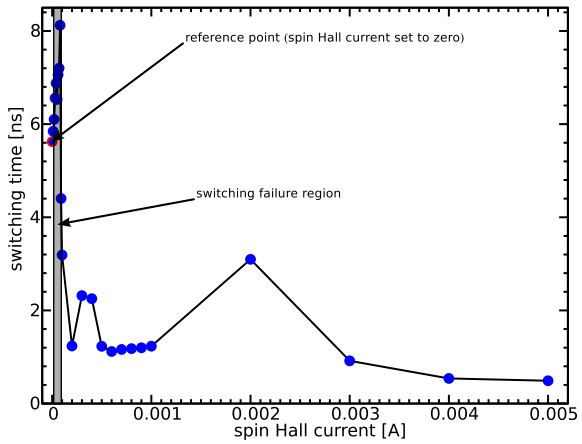

Fig. 3. Switching time as a function of applied spin Hall current at fixed pulse widths. Outside of the switching failure region the vortex excitation is still present (cf. two peaks), but does not cause switching failure.

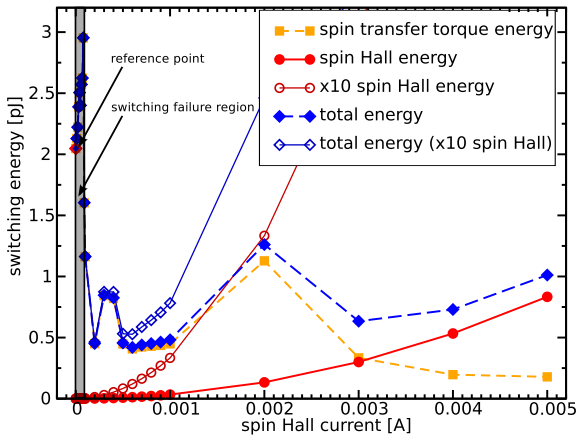

Fig. 4. Estimate of switching energy as a function of applied spin Hall current. Two different spin Hall energies are depicted. Filled symbols illustrate ideal leads to the device (no power consumed), while the empty symbols assume ten times elongated spin Hall metal lines to connect the device.

$\hbar$ denotes the Planck constant, μ_0 the magnetic permeability, J the applied current density, l the free layer thickness, M_S the magnetization saturation, P the spin current polarization, and $\vec{p}$ the unit polarization direction of the polarized current. The STT model for the magnetic tunnel junction exhibits an in-plane ($\vec{m} \times \vec{p} \times \vec{m}$) and a small out-of-plane component ($\vec{m} \times \vec{p}$).

The spin torque caused by the spin Hall effect is given by [14], [19]:

$$\vec{T}_{SH} = \frac{\hbar}{\mu_0 e} \cdot \frac{J_S}{l M_S} \cdot (\vec{m} \times \vec{p}_{SH} \times \vec{m} - \epsilon\, \vec{m} \times \vec{p}_{SH}) \quad (3)$$

$$J_S = \theta_{SH} \frac{I_C}{t_{HM}\, w_{HM}} \left(1 - \operatorname{sech}\left(\frac{\mathrm{t}_{HM}}{\lambda_{sf}}\right)\right) \quad (4)$$

$$\vec{p}_{SH} = \hat{\imath}_C \times \hat{\imath}_{SH} \quad (5)$$

J_S denotes the applied spin current density, $\vec{p}_{SH}$ the unit polarization direction of the polarized spin Hall current, ϵ the weighting of the non-adiabatic torque contribution, and θ_{SH} the spin Hall angle. Furthermore, I_C describes the applied charge current, t_{HM} the Hall metal thickness, w_{HM} the Hall metal width, and λ_{SF} the spin flip length. The unit polarization direction of the spin Hall current $\vec{p}_{SH}$ is given by the cross product of the unit direction of the charge flow $\hat{\imath}_C$ and the unit direction of the spin flow $\hat{\imath}_{SH}$.

The switching energy for the spin transfer torque pulse is estimated as follows:

$$W_{STT} = I^2\, R_{MTJ}\, \Delta t = 2 \cdot j^2\, a^2\, \mathcal{RA}\, t_{switch} \quad (6)$$

I describes the applied current, R_{MTJ} the average stack resistance, Δt the pulse length, $\mathcal{RA}$ the area resistance product of the tunnel oxide, and t_{switch} the required switching time ($\Delta t = t_{switch}$). The right hand side term is gained by substituting $I \rightarrow j2\,a^2$ and $R_{MTJ} \rightarrow \mathcal{RA}/(2a^2)$.

The employed switching energy for the spin Hall pulse is estimated by the energy dissipated in the Hall metal lines:

$$W_{SH} = I_{SH}^2\, R_{SH}\, \Delta t_{SH} = I_{SH}^2\, \rho_{SH}\, \frac{l_{HM}}{t_{HM}\, w_{HM}} \Delta t_{SH} \quad (7)$$

I_{SH} denotes the charge current through the wire, R_{SH} the wire resistance, ρ_{SH} the resistivity of the wire, l_{HM} the wire length, and Δt_{SM} the pulse length.

IV. Results and Discussion

The data points marked with a red border shown in Fig. 3 and Fig. 4 depict the average of simulations without spin Hall pulses and serve as a reference for comparison against the influence of the spin Hall current amplitude on the switching time and energy. Plotting the switching time as a function of the applied current to the metal lines shows two regimes (see Fig. 3) - a switching failure region and an operational region. One can see that initially, when the spin Hall current increases, there is a steep rise in switching time, followed by a fast drop around 80μA and two more hillocks which are far less pronounced than the first one. The same trend can be observed, if one looks at the standard deviation of the

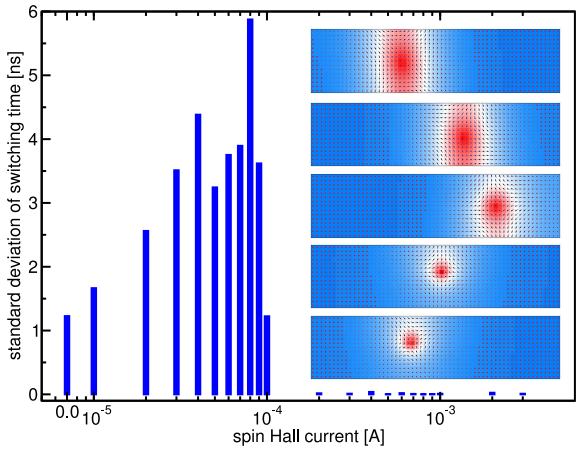

Fig. 5. Standard deviation of the switching times as a function of spin Hall current. The effect of the vortex excitation is also shown by the steep broadening of the switching time distribution width. The inset illustrates the formation of a vortex in the free layer and its movement during switching.

corresponding points as a function of spin Hall current (cf. Fig. 5). In order to understand the reason for this, we checked the position and time dependent evolution of the free layer magnetization for low currents and found the formation of vortices during the switching process (see inset of Fig. 5). The vortices wander through the free layer and do not only delay the switching significantly but also can cause switching failure. Starting with $100\mu\mathrm{A}$ the vortex excitations stop to cause failures, but are still present as can be seen by the two peaks visible in Fig. 3. Outside of the failure region the switching time can be reduced between a factor of five ($1.12\mathrm{ns}$ at $600\mu\mathrm{A}$) and two ($3.1\mathrm{ns}$ at $2\mathrm{mA}$) in comparison to the reference point ($5.62\mathrm{ns}$ at $0A$). Fig. 4 illustrates the estimated switching energy for the proposed device as a function of the applied spin Hall current. The spin transfer torque contribution to the switching energy is directly proportional to the switching time due to the fixed applied current density and fixed stack resistance (cf. Fig. 3). On the other hand the spin Hall energy contribution is proportional to the spin Hall current squared, since the resistance as well as the pulse time were fixed. If one now compares the switching energy reference point against the total switching energy estimates for ideal leads, where only in the region adjacent to the free layer power is dissipated, and non-ideal leads, where the length of the spin Hall metal line l_{HM} is ten times elongated, there is a region where not only the switching is accelerated, but also the overall switching energy is significantly reduced (between $300\mu\mathrm{A}$ and $2\mathrm{mA}$). The achievable energy reduction lies between a factor of approximately five ($\approx 0.42\mathrm{pJ}$) and 1.6 ($\approx 1.26\mathrm{pJ}$) for ideal leads, respectively. This demonstrates that the use of the SHE is rewarded by a simultaneous boost in switching time and switching energy reduction. Furthermore, it allows to decrease the wear of the tunneling oxide and does not degrade the thermal stability of the device.

V. Conclusion

We have shown that the switching energy is reduced and the speed of the proposed non-volatile flip flop is significantly enhanced by employing the spin Hall effect without a detrimental side effect on the thermal stability. This is achieved by placing the flip flop structure on two spin Hall metal lines and performing two short pulses through the lines, before the actual flip flop operation. The simulations show that the use of the spin Hall effect is rewarded by a simultaneous reduction in switching time ($\times 5 - \times 2$) and switching energy ($\times 5 - \times 1.6$).

Acknowledgment

This work is supported by the European Research Council through the grant #247056 MOSILSPIN.

References

[1] (2013) International Technology Roadmap for Semiconductors, Chapter PIDS. [Online]. Available: http://www.itrs.net/Links/2013ITRS/Home2013.htm

[2] N. Kim, T. Austin, D. Baauw, T. Mudge, K. Flautner, J. Hu, M. Irwin, M. Kandemir, and V. Narayanan, "Leakage Current: Moore's Law Meets Static Power," *Computer*, vol. 36, no. 12, pp. 68–75, 2003.

[3] D. Nikonov and I. Young, "Overview of Beyond-CMOS Devices and a Uniform Methodology for Their Benchmarking," *Proceedings of the IEEE*, vol. 101, no. 12, pp. 2498–2533, 2013.

[4] A. Makarov, V. Sverdlov, and S. Selberherr, "Emerging Memory Technologies: Trends, Challenges, and Modeling Methods," *Microelectronics Reliability*, vol. 52, no. 4, pp. 628–634, 2012, Advances in Non-Volatile Memory Technology.

[5] Everspin Technologies, Jul. 2015. [Online]. Available: http://www.everspin.com/mram-replaces-dram

[6] S. Ikeda, K. Miura, H. Yamamoto, K. Mizunuma, H. D. Gan, M. Endo, S. Kanai, J. Hayakawa, F. Matsukura, and H. Ohno, "A Perpendicular-Anisotropy $CoFeB - MgO$ Magnetic Tunnel Junction," *Nat. Mater.*, vol. 9, pp. 721–724, Sep. 2010.

[7] K. Abe, H. Noguchi, E. Kitagawa, N. Shimomura, J. Ito, and S. Fujita, "Novel Hybrid DRAM/MRAM Design for Reducing Power of High Performance Mobile CPU," in *Electron Devices Meeting (IEDM), 2012 IEEE International*, 2012, pp. 10.5.1–10.5.4.

[8] H. Yoda, S. Fujita, N. Shimomura, E. Kitagawa, K. Abe, K. Nomura, H. Noguchi, and J. Ito, "Progress of STT-MRAM Technology and the Effect on Normally-Off Computing Systems," in *Electron Devices Meeting (IEDM), 2012 IEEE International*, 2012, pp. 11.3.1–11.3.4.

[9] W. Zhao, L. Torres, Y. Guillemenet, L. V. Cargnini, Y. Lakys, J.-O. Klein, D. Ravelosona, G. Sassatelli, and C. Chappert, "Design of MRAM Based Logic Circuits and its Applications," in *ACM Great Lakes Symposium on VLSI*, 2011, pp. 431–436.

[10] T. Windbacher, H. Mahmoudi, V. Sverdlov, and S. Selberherr, "Rigorous Simulation Study of a Novel Non-Volatile Magnetic Flip Flop," in *Proc. of the SISPAD*, 2013, pp. 368–371.

[11] M. I. D'Yakonov and V. I. Perel', "Possibility of Orienting Electron Spins with Current," *ZhETF Pisma*, vol. 13, no. 11, pp. 657–660, Jun. 1971.

[12] Y. K. Kato, R. C. Myers, A. C. Gossard, and D. D. Awschalom, "Observation of the Spin Hall Effect in Semiconductors," *Science*, vol. 306, no. 5703, pp. 1910–1913, 2004.

[13] T. Kimura, Y. Otani, T. Sato, S. Takahashi, and S. Maekawa, "Room-Temperature Reversible Spin Hall Effect," *Phys. Rev. Lett.*, vol. 98, p. 156601, Apr. 2007.

[14] Y. Kim, X. Fong, K.-W. Kwon, M.-C. Chen, and K. Roy, "Multilevel Spin-Orbit Torque MRAMs," *Electron Devices, IEEE Transactions on*, vol. 62, no. 2, pp. 561–568, Feb 2015.

[15] C.-F. Pai, L. Liu, Y. Li, H. W. Tseng, D. C. Ralph, and R. A. Buhrman, "Spin Transfer Torque Devices Utilizing the Giant Spin Hall Effect of Tungsten," vol. 101, no. 12, pp. –, 2012.

[16] T. Windbacher, H. Mahmoudi, V. Sverdlov, and S. Selberherr, "Novel MTJ-Based Shift Register for Non-Volatile Logic Applications," in *Proceedings of the 2013 IEEE/ACM International Symposium on Nanoscale Architectures*, 2013, pp. 36–37, (NANOARCH), New York City, USA; 2013-07-15 – 2013-07-17.

[17] U. Tietze and C. Schenk, *Electronic Circuits – Handbook for Design and Applications*, 2nd ed. Springer, 2008, no. 12.

[18] A. Lyle, X. Yao, F. Ebrahimi, J. Harms, and J.-P. Wang, "Communication Between Magnetic Tunnel Junctions Using Spin-Polarized Current for Logic Applications," *Magnetics, IEEE Transactions on*, vol. 46, no. 6, pp. 2216–2219, June 2010.

[19] S. Manipatruni, D. Nikonov, and I. Young, "Energy-Delay Performance of Giant Spin Hall Effect Switching for Dense Magnetic Memory," *Applied Physics Express*, vol. 7, no. 10, p. 103001, 2014.

[20] T. Gilbert, "A Lagrangian Formulation of the Gyromagnetic Equation of the Magnetization Field." *Phys. Rev.*, vol. 100, p. 1243, 1955.

[21] H. Kronmüller, *Handbook of Magnetism and Advanced Magnetic Materials*. John Wiley & Sons, Ltd, 2007, ch. General Micromagnetic Theory.

[22] J. E. Miltat and M. J. Donahue, *Handbook of Magnetism and Advanced Magnetic Materials*. John Wiley & Sons, Ltd, 2007, ch. Numerical Micromagnetics: Finite Difference Methods.

[23] W. F. Brown, "Thermal Fluctuations of a Single-Domain Particle," *Phys. Rev. B*, vol. 130, pp. 1677–1686, Jun 1963.

[24] K. Ito, T. Devolder, C. Chappert, M. J. Carey, and J. A. Katine, "Probabilistic Behavior in Subnanosecond Spin Transfer Torque Switching," *J.Appl.Phys.*, vol. 99, no. 8, 2006.

[25] J. C. Slonczewski, "Currents, Torques, and Polarization Factors in Magnetic Tunnel Junctions," *Phys. Rev B*, vol. 71, p. 024411, Jan 2005.